Amino Acid Sequence of Oligopeptide Causes Marked Difference in DNA Compaction and Transcription

A. Zinchenko, H. Hiramatsu, H. Yamaguchi, K. Kubo, S. Murata, T. Kanbe, N. Hazemoto, K. Yoshikawa, T. Akitaya

Abstract

Compaction of T4 phage DNA (166 kbp) by short oligopeptide octamers composed of two types of amino acids, four cationic lysine (K) and four polar non-ionic serine (S) having different sequence order was studied by single-molecule fluorescent microscopy. We found that efficient DNA compaction by oligopeptide octamers depends on the geometrical match between phosphate groups of DNA and cationic amines. The amino acid sequence order in octamers dramatically affects the mechanism of DNA compaction which changes from a discrete all-or-nothing coil-globule transition induced by less efficient (K_4S_4) octamer to a continuous compaction transition induced by $(KS)_4$ octamer with a stronger DNA-binding character. This difference in the DNA compaction mechanism dramatically change the packaging density and the morphology of T4 DNA condensates: DNA is folded into ordered toroidal or rod morphologies during all-or-nothing compaction, whereas disordered DNA condensates are formed as a result of the continuous DNA compaction. Furthermore, the difference in DNA compaction mechanism has a certain effect on the inhibition scenario of the DNA transcription activity, which is gradual for the continuous DNA compaction and abrupt for the all-or-nothing DNA collapse.

Keywords

DNA compaction, single-molecule microscopy, oligopeptide, transcription

Introduction

A long genomic DNA must be compacted to fit within a minute space of a cell nucleus or bacteriophage capsid head. This process *in vivo* is assisted by proteins and polyamines and results in more than 1000-fold decrease of DNA molecular volume compared to the size of DNA coil in aqueous solutions corresponding to DNA packing densities of 400−500 mg/mL. In sperm nuclei, DNA is compacted by small, highly positively charged, arginine rich peptides called protamines (1). In eukaryotes, DNA tightly wraps around cationic proteins, histones, (2-4) and form compact chromatin fibers. Histones possess both cationic and anionic groups on their surface and the spatial distribution of charges, determined by amino acids sequence, plays crucial role in the stabilization of the compact forms of DNA in the DNA-histone complex.(5) DNA-binding motifs of high-mobility group B (HMGB) proteins, regulating DNA-dependent processes such as transcription, replication, recombination, and DNA repair, consist of a few cationic amino acid residues like histone. Such cationic amino acid sequences are effective to bind, bend and/or compact DNA chain, however precise mechanisms related to sequences still remain unclear (6-9).

Controllable DNA compaction via structural design of effective gene transfer vectors is an important for various biomedical applications such as gene therapy.(10, 11) Cationic oligo- and polypeptides containing cationic lysine and arginine amino acids are recognized as essential components of *in vitro* systems to condense and deliver DNA into living cells (12). Cationic polypeptides neutralize DNA negative charge and form compact polyelectrolyte complexes with DNA target (13, 14) favoring interaction of the DNA-peptide complexes with the cell membrane and consequent facile internalization of DNA into cell (15). Varying of amino acids chemistry, sequence, polypeptide chain length, etc. was used to optimize DNA compaction and transfection efficiency of DNA-polypeptide complexes (16, 17).

DNA compaction phenomenon *in vitro* has been intensively studied theoretically and experimentally for many decades to unveil driving forces leading to the formation of condensed DNA *in vivo* (18-21). It was argued experimentally (22) and theoretically (23) that, generally, cationic binders with a charge +3 and higher induce sufficient DNA charge neutralization that results in DNA compaction. Polylysines and polyarginines with more than three cationic monomer units were shown to induce DNA compaction (24-26) and structural factors of peptides controlling DNA compaction were analyzed (Table 1). Tri-arginine is more efficient than tri-lysine in terms of polypeptide concentration and packaging density of DNA in condensates (24). Difference in chirality of tri-lysines and tri-arginine also caused a profound change in their DNA compaction potentials (24). Increase of polypeptide length results in more efficient DNA compaction in terms of polypeptide concentration (26). Compaction mechanism of DNA changes from very cooperative transition in case of short oligopeptides to a continuous compaction by longer polypeptide chains (26). Length of polypeptides and the charge ratio between DNA and polypeptide has clear effect on the morphology of the condensed DNA molecules (27, 28).

Table 1. Comparison of DNA compaction efficiencies of various cationic peptides

Studied polypeptides	Comparison of DNA compaction efficiency
Amino acid composition of homo-oligopeptides	Arg_3 > Lys_3 (24), polyArg > polyLys (26)
Polypeptide length	polyLys > Lys_9 > Lys_3 (26)[1]
Placement of two types of cationic amino acids in oligopeptide	Arg_3Lys_3 ≈ Lys_3Arg_3 (29)[2]
Insertion of neutral amino acids in a sequence of cationic oligopeptide	Arg_6 > $Arg_3AlaArg_3$ > $Arg_3Ala_2Arg_3$ (30)[2]
Placement of cationic and neutral amino acids in oligopeptides	Arg_3Ala_3 ≈ Ala_3Arg_3 (30)[2]
DNA sequence effect on compaction by Lys_6	TT ≥ TA ≈ mCG > UA ≥ CG > CC (31)[2]

[1] In terms of monomer units' concentrations
[2] Based on DNA-DNA interchain distance estimated through osmotic stress technique

Less is known about the effect of amino acid sequence in oligopeptides having the same charge on DNA compaction. Rau et al. studied DNA packaging by two hexapeptides Arg_3-Lys_3^{6+} and Arg-Lys-Arg-Lys-Arg-Lys^{6+} and concluded that placement of the charged groups does not affect DNA attraction forces (29). In their further works it was shown that insertion of neutral or anionic amino acids between charged lysines results in a significant decrease of an attraction between DNA helixes suggesting negative effect on DNA compaction efficiency (30). Interestingly, position of non-charged groups in oligopeptides with the same amino acid contents was shown to slightly change the attraction potentials between DNA chains (30). On the other hand, not only peptide sequence but also AT/GC contents of DNA was shown to be important. For example, TA-rich DNA constructs are condensed by Lys_6 or spermine more efficiently than CG-rich ones (31).

As shown above, whereas the importance of amino acid sequence in DNA compaction and transfection was acknowledged (11, 32), to the best of our knowledge, there have been no careful investigations on the effect of oligopeptide sequence order on the higher-order structural behavior of DNA molecules and morphology of DNA condensates formed through interaction with polypeptides. Here, we prepared peptide octamers composed of cationic lysine and non-ionic polar serine amino acids to study the compaction of a long genomic DNA induced by these multivalent cations. We found that sequence order of amino acids in oligopeptide, that shows a moderate influence on DNA compaction efficiency, dramatically affects the DNA compaction scenario at the level of single DNA chains and structure of thereby formed DNA condensates. Finally, DNA compaction scenario significantly influences the inhibition profile of DNA transcriptional activity during compaction.

Experimental section

Materials

T4 phage DNA composed of *ca.* 166 kbp with a contour length of ca. 60 μm was purchased from Nippon Gene Co., Ltd. (Toyama, Japan). DAPI fluorescent dye (4′,6-diamidino-2-phenylindole dihydrochloride) was purchased from Wako Pure Chemicals Industries, Ltd. (Osaka, Japan). Tris-HCl buffer solution (1 M, pH 7.6) and 2-mercaptethanol were purchased from Nacalai Tesque Inc. (Japan). Deionized water (Milli-Q, Millipore) was used for preparing samples.

Monomeric amino acids precursors Fmoc-Lys(Boc)-OH and Fmoc-Ser(tBu)-OH were purchased from Nova Biochem (Darmstadt, Germany) and peptide octamers were synthesized according to the fluoren-9-yl-methoxycarbonyl (Fmoc) procedure (33) using a peptide synthesizer (model 431A, Applied Biosystems, Foster City, CA).

Ribonucleoside triphosphates (NTP: ATP, CTP, GTP, and UTP) (Roche Diagnostics), sterile-filtered and autoclaved 5 M NaCl and 1 M $MgCl_2$ solutions (Nacalai Tesque, Inc.), 0.1 M dithiothreitol (DTT) (Invitrogen), sterile and autoclaved DNase and RNase free distilled water (Nippon Gene Co., Ltd.), DNase and RNase free TE-saturated phenol solution (Nippon Gene Co.,Ltd.), nuclease and protease tested sodium acetate (Nacalai Tesque, Inc.), glycogen (Roche Diagnostics), ethanol (99.5%) (Nacalai Tesque, Inc), and RiboGreen RNA Quantitation Kit (Molecular Probes, Inc.) were used for transcription experiments.

Methods

Fluorescence Microscopy

Fluorescence images of T4 phage DNA solution (0.2 μM in phosphates) in 10 mM Tris-HCl buffer (pH 7.6) stained with a fluorescent dye DAPI (0.1 μM) and in the presence of radical scavenger 2-mercaptethanol (4% v/v) were directly observed at room temperature using an Axiovert 135 TV microscope (Carl Zeiss AG) and recorded on SIT TV camera C2400-8 (Hamamatsu Photonics Co. Ltd.) through Argus 10 image processor (Hamamatsu Photonics,

Hamamatsu, Japan). DNA long-axis length, the longest distance in the fluorescence image of single DNA molecules, was measured on 50-100 randomly selected DNA molecules using the image analysis software Cosmos (Library, Tokyo, Japan).

Transmission electron microscopy (TEM)

TEM observations were performed at room temperature on a JEOL JEM-1400EX Electron Microscope (JEOL Ltd., Japan) at 200 kV acceleration voltage. 3 mm carbon-coated copper grid was placed on 10 μL droplet of T4 DNA solution (0.8 μM in phosphates) containing appropriate amount of peptide octamers on a Parafilm sheet and incubated for 2-3 minutes. Then, the solution was blotted with a filter paper and the grid was placed for 1-2 min on a 10 μL droplet of uranyl acetate (1% in water) for staining prior to final blotting and microscopic observation.

Measurements of DNA transcriptional activity

LambdaGEM-11 DNA (43 kbp, Promega) including a T7 promoter was used as a template for transcription by T7 RNA polymerase (T7 RNAP; Invitrogen, Gaithersburg, MD). For the control experiment, 472 bp fragments including T7 promoter were prepared by polymerase chain reaction (Takara Taq Hot Start; Takara Shuzo, Otsu, Japan) using LambdaGEM-11 DNA as a template and a set of synthesized primers (forward 5'-AAGGTAGGOGGATCTGGGTC-3' and reverse 5'-OGAGGTTGCAAACCATC-3'). After purification, the monodispersity of PCR products was confirmed by electrophoresis on agarose gel. Transcription was performed in 50 mL reaction solutions containing 10 mM Tris–HCl buffer (pH 7.6), 100 mM NaCl, 5 mM $MgCl_2$, 0.5 mM NTPs, and 5 mM DTT. After adding 50 U of T7 RNAP, the solution was incubated at 37 °C for 1-1.5 h. The reaction was stopped by adding Tris-saturated phenol. RNA products and DNA templates were recovered by ethanol precipitation, dried and rehydrated with distilled water. The DNA templates were then digested with 1 U of deoxyribonuclease (Wako Nippon Gene, Tokyo, Japan) at 37 °C for 1.5 h. The samples were stained by adding

an equal volume of 200-fold diluted RiboGreen dye in Tris-EDTA (TE) buffer, and the fluorescence intensity was measured using a spectrofluorimeter as describer in details elsewhere (34).

Prediction of octamers secondary structure

The secondary structure of studied octamers was analyzed using a calculation program, CRNPRED (https://pdbj.org/crnpred/), for predicting secondary structures, contact numbers, and residue-wise contact orders of native protein structure using critical random networks (35). The calculations were performed at the most accurate CRN5000 level based on 5000-dimensional state vectors. The results of secondary structure prediction obtained by CRN5000 have been also confirmed by JPred4 protein secondary structure prediction program (http://www.compbio.dundee.ac.uk/jpred4) and the predicted conformations of the polypeptides by both simulations were identical.

Results and Discussion

The structures of oligopeptide octamers used for DNA compaction experiments are shown in **Figure 1**. Each of oligopeptide molecules contains four cationic lysin (K) and four non-ionic hydrophilic serine (S) amino acid residues connected in either block (KKKKSSSS = K_4S_4 and KKSSKKSS = $(K_2S_2)_2$) or alternating (KSKSKSKS = $(KS)_4$) order.

Compaction of bacteriophage T4 DNA (166 kbp, contour length *ca.* 60 μm) by peptide octamers (**Figure 1**) was studied by fluorescence microscopy (FM) at the level of single DNA molecules. T4 DNA was labeled with a DAPI fluorescent dye and its conformational dynamics in a bulk solution was monitored and analyzed (**Figure 2**). In buffer solution, individual DNA molecules adopted a fluctuating coil conformation with the average long-axis length of *ca.* 4 μm and exhibited a free Brownian motion both for the intramolecular conformation and the translational motion. Addition of either peptide octamer into solution of DNA induced a

conformational transition of DNA molecules from an unfolded coil to a compact globule conformation. **Figure 2A** illustrates the evolution of single T4 DNA molecules state from coil, to coil-globule co-existence state, and to globule state upon addition of K_4S_4 octamer; and from coil, to shrunken coil state, and to globule state upon addition of $(KS)_4$ octamer (**Figure 2B**). DNA globules were

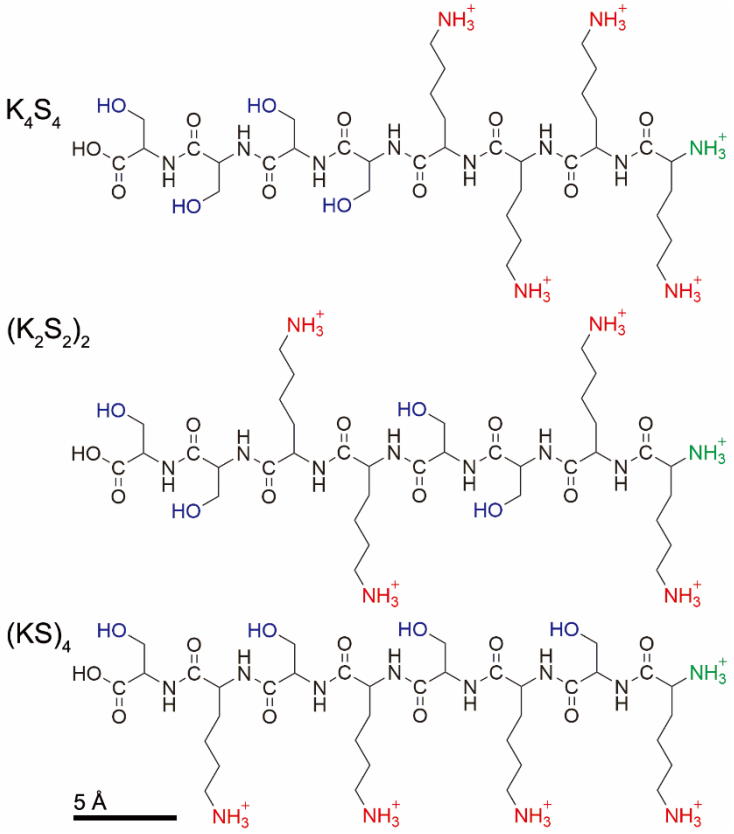

Figure 1. Oligopeptide octamers. Molecular structures of K_4S_4, $(K_2S_2)_2$, and $(KS)_4$ peptide octamers used as DNA compaction agents. Protonated ε-amino groups are shown in red and N-terminal amines in green.

observed as quickly moving compact particles with the apparent size of *ca.* 0.6-0.7 μm. The actual size of compact DNA is smaller by *ca.* 0.3 μm in each dimension due to the "blurring effect" discussed elsewhere (36). Size distributions of DNA at different concentrations of peptide octamers were built by measuring the long-axis length of individual DNA molecules (**Supporting Information, Figures S1, S2, and S3**). DNA compaction potentials of K_4S_4, $(K_2S_2)_2$, and $(KS)_4$ were compared by plotting the average values of DNA long-axis length as

a function of oligopeptide concentration (**Figure 2C-D**). DNA compaction by $(KS)_4$ with an alternating order of lysine and serine amino acids was the most efficient and took place at $(KS)_4$ concentration of 40 μM. Other two octamers induced DNA compaction at higher concentrations, and the order of DNA compaction potentials among studied octamers was K_4S_4, < $(K_2S_2)_2$ < $(KS)_4$.

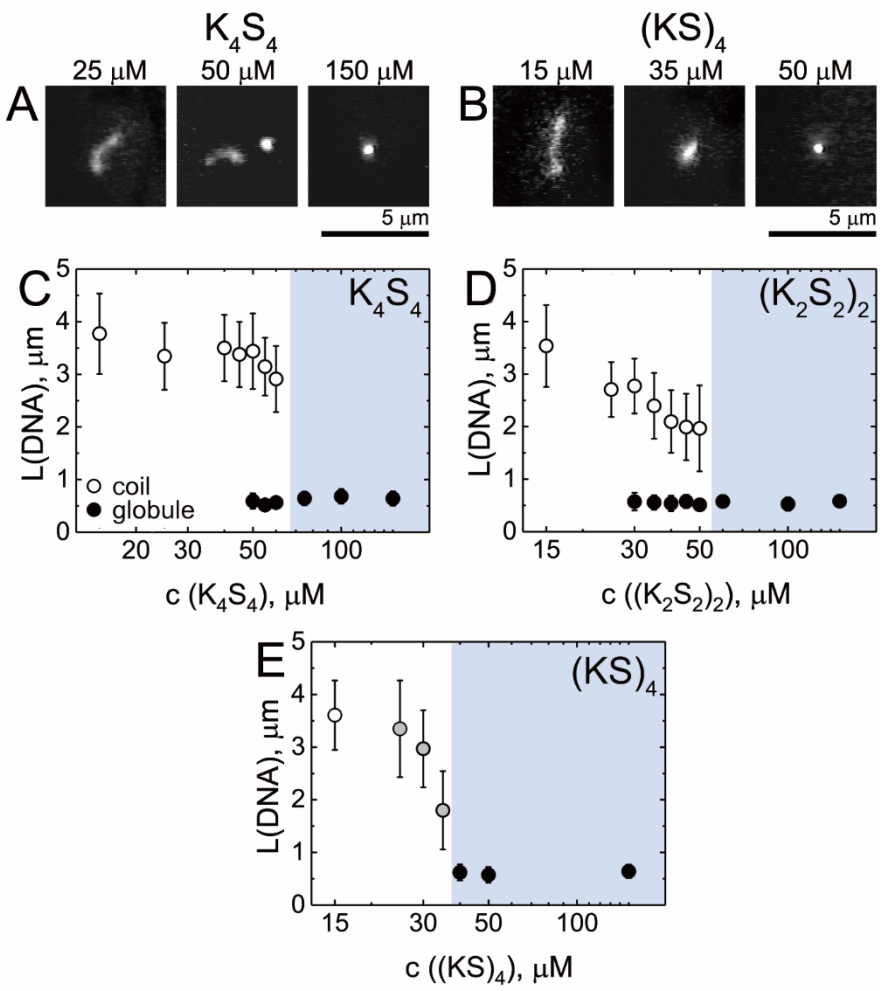

Figure 2. Fluorescence microscopy observation of T4 DNA molecules compaction by peptide octamers. A. Fluorescence images of single T4 DNA in a coil, coexistence, and globule conformational states in solutions at different K_4S_4 concentration. **B.** Fluorescence images of T4 DNA in a coil, shrunken coil, and globule conformational states in solutions at different $(KS)_4$ concentrations. **C-E.** Changes in the average long-axis length of T4 DNA (0.2 μM in phosphates) as a function of K_4S_4 (**C**), $(K_2S_2)_2$ (**D**), and $(KS)_4$ (**E**) concentrations. Shaded areas on graphs indicate DNA globule state. DNA long-axis length values shown by grey symbols were averaged over both coil and globule DNA conformations. The error bars are standard deviations of the average long-axis length values measured over 50-100 individual DNA molecules.

To explain the observed difference between octamers' efficiency in DNA compaction, we assume that geometry matching of DNA phosphate groups and oligopeptide amino groups plays a pivotal role in DNA charge neutralization – the main driving force of DNA compaction. Previous studies showed that compaction of DNA is generally induced by cationic species having the formal charge +3 and higher (22, 37), but di- and even monovalent cations having hydrophobic substituents can strongly promote DNA collapse (38, 39). The correlation between cationic charge of DNA-binding molecule and DNA compaction efficiency was also demonstrated for polyamines (40) and cationic polypeptides (26). In case of organic multivalent cations, spatial mismatch between cationic and anionic groups originated due to difference between intercharge distances in a multication and inter-phosphate distances in DNA (39, 41, 42) results in less effective DNA compaction. On the example of organic diammonium salts, earlier we demonstrated that the geometry fit between cationic groups of dications and phosphate groups of DNA is essential for the efficient DNA charge neutralization and compaction (39). Furthermore, photochemical control of an intercharge distance in photosensitive dications was successfully utilized to reversibly induce DNA compaction and decompaction (43) supporting the model based on ionic pairs formation for the efficient DNA compaction. DNA compaction by branched multications is less efficient compared to linear ones due to unavailability of a part of cationic groups for DNA binding (44).

To make clear the origin of more efficient DNA compaction by $(KS)_4$ octamer, we analyzed the molecular geometry of peptides and DNA in B-form by a molecular modeling program using standard parameters for bond lengths and angles. Preliminary analysis of octamers' secondary structure performed by CRNPRED method (35) indicated that all studied oligopeptides existed in a random coil conformation (**Supporting information, Table S1, S2 and S3**). Thus, the effect of oligopeptide secondary structure formation on spatial arrangements of charges can be neglected. **Figure 3** shows molecular models of oligopeptides K_4S_4, $(K_2S_2)_2$,

and $(KS)_4$ together with the values of longest distances between the most distant cationic amino groups in the molecules. Each octamer contains four ε-amino groups and one N-terminate amine, which is partially protonated (pK_a = 8.0) in buffer solution (pH = 7.6) and is also considered to take part in ionic bond formation with DNA phosphates.

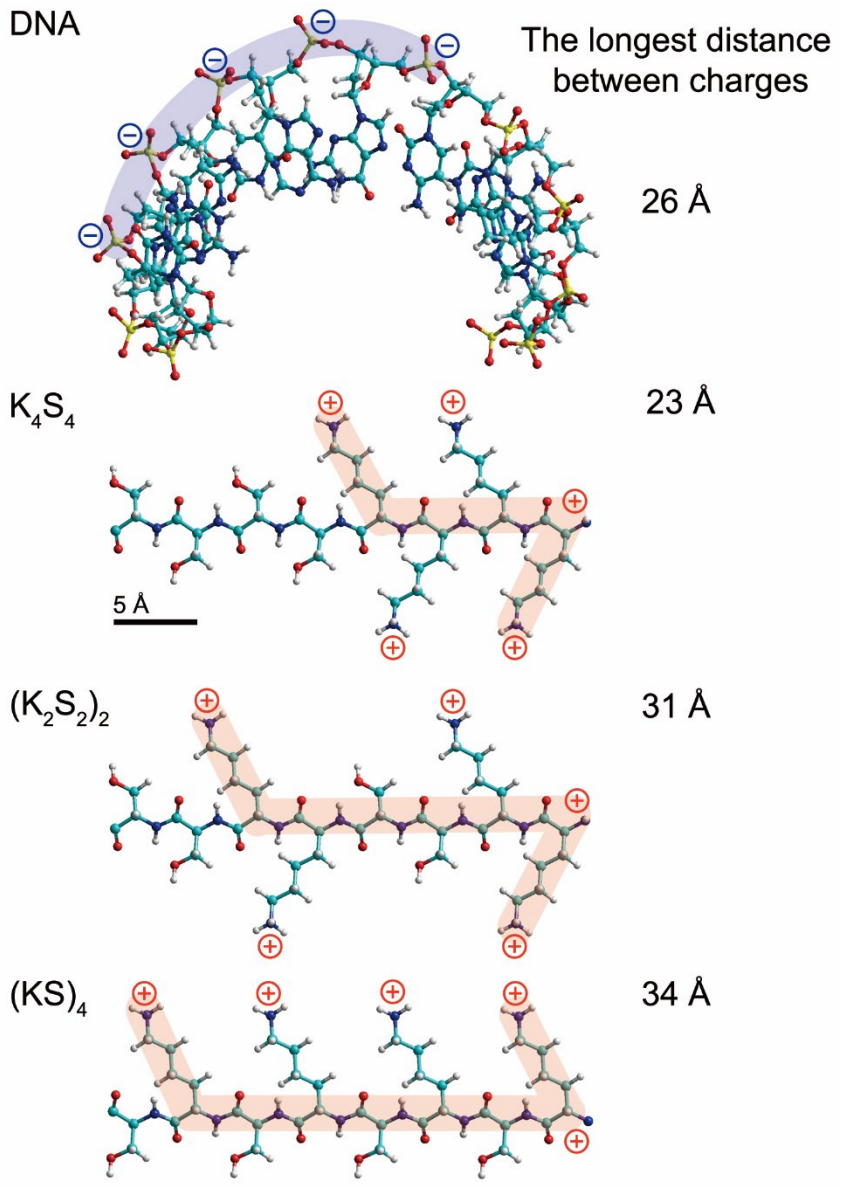

Figure 3. Intercharge distance in DNA and peptide octamers. Schematic representation of spatial arrangement of phosphate groups on DNA (only a single-stranded fragment on double-stranded DNA is shown) and the amines in peptide octamers, and the values of distances between the most distant charges. The longest distance between 5 DNA charges was calculated as a sum of four average inter-phosphate distances using average standard parameters of bonds lengths and angles of double-stranded DNA in B-form. The longest distance between charged amino groups in peptide octamers was estimated as a sum of distances along the shadowed path

on the corresponding oligopeptide images using standard parameters of bond lengths and angles. The hydrogen atoms of N-terminal amino groups are not shown.

By molecular dynamic simulations it was shown that basic side chains of peptides interacting with DNA phosphates are relatively mobile even after formation of ionic pairs with DNA phosphates.(45) Therefore, five ionic pairs with DNA phosphates can be potentially formed. However, accessibility of five adjacent DNA phosphate groups to the amines of peptide octamers depends on their molecular structure. For example, average distance between phosphate groups in DNA in B-form is *ca.* 6.5 Å, that corresponds to *ca.* 26 Å contour distance between first and fifth phosphates, but the longest distance between amino groups in K_4S_4 is only 23 Å (**Figure 3**); therefore, 5 ionic pairs ($NH_3^+ PO_4^-$) cannot be efficiently formed. The longest distance between cationic groups in $(K_2S_2)_2$, and $(KS)_4$) are 31 Å and 34 Å, respectively suggesting that there are no steric obstacles for the formation of 5 ionic pairs. The above consideration on the electrostatic neutralization of DNA phosphates by amines in the peptide octamers suggests higher DNA binding constants for $(KS)_4$ than K_4S_4, and, consequently, higher DNA compaction potential of $(KS)_4$ that was confirmed in the FM experiments (**Figure 2**). Similar experimental trend was reported by Thomas et al. in their study of DNA condensation by tetraamines having different intercharge distance between two central amino groups (42). First, it was clearly demonstrated that tetraamine with the closest arrangement of cationic groups is not the most potent for DNA compaction. Second, in a good agreement with our model, it was found that there was an optimal intercharge distance between amines that roughly correspond to a situation when the length of polyamine molecule was sufficient for terminate amines separated by 18.5 Å distance to reach the first and the forth DNA phosphates in a sequence separated by 19.5 Å distance.

A number of past studies considered other models of DNA-polypeptide structural recognition (46). According to theoretical studies of Kornyshev and Leikin, the ability of polypeptide to

bind into DNA groove may be associated with a higher DNA compaction potency (47). Other research groups advocated for the importance of the ability of DNA binder to form bridges between DNA strands to promote DNA condensation. Influence of polyamine length on DNA-DNA strand separation in condensates was studied by X-ray techniques and it was shown that DNA-DNA interhelical distance increases with an increase of the bulkiness of DNA binder. Based on these results the bridging model for multication interaction with DNA was proposed (48). Finally, in contrast to model considering cation binding specificity, there have been studies that treated DNA condensation problem purely in terms of counterion-induced electrostatic attraction between like charged rods of DNA helixes (46), also known as "electrostatic zipper model" (47). In particular, peptide sequence homology effect on charge distribution along DNA cylinders was investigated as possible factor promoting attraction between two DNA helixes (49).

It is important to note that binding affinity of a peptide to DNA does not always correlate with their DNA compaction efficiency. For example, incorporation of tryptophan into oligopeptides containing several lysine or arginine moieties had no major effect on DNA binding affinity but clearly reduced the DNA compaction potency of the peptides (32).

Importantly, although we observed a moderate difference between the concentrations of K_4S_4, $(K_2S_2)_2$ or $(KS)_4$ at which DNA compaction occurred, there was a striking effect on the scenario of DNA compaction transition (**Figures 2**). Compaction of DNA by K_4S_4, $(K_2S_2)_2$ occurred as a first-order phase transition at the level of individual DNA chains during which the conformation of DNA abruptly changed from coil to globule skipping any intermediate, partially folded, states. In contrast, compaction of DNA by $(KS)_4$ was a continuous transition characterized by a gradual DNA long-axis length toward the formation of fully compact DNA condensate.

It is well established that compaction of sufficiently long DNA molecules (>10 kbp) by tri- or tetracations such as spermine or spermidine is a discrete transition of DNA from coil into globule (50). On the example of polylysines having different polymerization degree, it was shown that DNA compaction scenario changed from discrete transition to continuous transition when the cationicity of polypeptide increased up to *ca.* 10 cationic monomers per one polylysine molecule (26). This switch in DNA compaction scenario due to an increase in DNA binder cationicity was explained based on attraction/repulsion interactions of DNA segments along single DNA (51, 52). In case of weakly charged cationic binders, interaction between DNA segments is predominantly repulsive and the compaction of DNA occurs in a very abrupt manner when the threshold of cationic species concentration in DNA solution is reached. In contrast, stronger binding of DNA to more cationic polyamines turns the interaction between DNA segments to attractive that enables the formation of various partially compact DNA conformations that, in turn, results in a continuous nature of DNA compaction. The switch of DNA compaction mechanism observed for the studied oligopeptides (**Figure 2**) satisfactorily agrees with the above model. Geometry matching of DNA phosphate groups and oligopeptide amino groups may greatly contribute to charge neutralization of DNA because a moderate difference was observed between K_4S_4 and $(K_2S_2)_2$ or $(KS)_4$ whereas a great difference between oligo-L-lysine less than 10-mer and poly-L-lysine was reported (12). Indeed, an increase of the DNA-binding character from K_4S_4 to $(KS)_4$ leads to a transition from all-or-nothing DNA compaction scenario to a continuous compaction scenario.

There are many literature examples pointed to the morphological difference between DNA condensates as a result of variation in the charge (53), branching degree (54), chirality (24), and other structural parameters of polycationic binder. Not surprisingly, we found that the variation in DNA compaction mechanism between first-order phase transition and a continuous transition originated clear morphological changes of DNA condensates. Compact DNA

condensates formed in solutions of K_4S_4 and $(KS)_4$ at concentrations slightly exceeding the DNA collapse concentrations were visualized by transmission electron microscopy (TEM) (**Figure 4**).

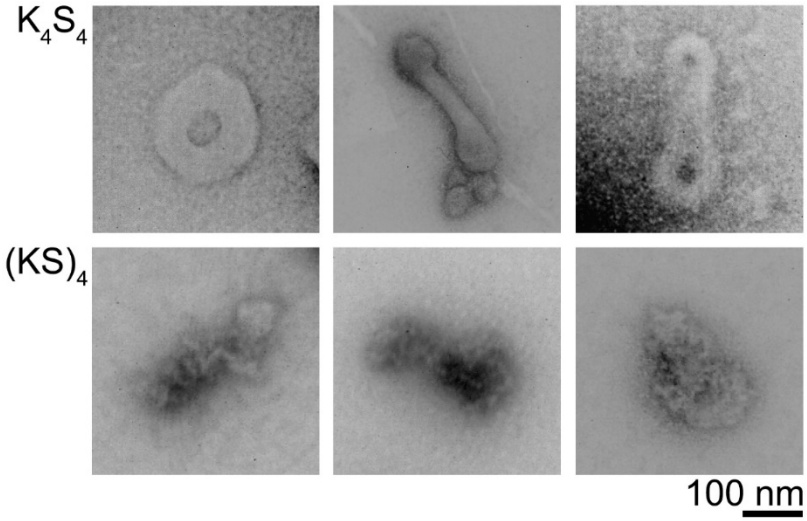

Figure 4. Morphology of single DNA condensates Transmission electron microscopy images of single T4 DNA molecules condensed in the presence of K_4S_4 and $(KS)_4$ at 150 μM concentration.

The dimension of compact T4 DNA condensates formed in solutions of either condensing agent was 100-200 nm in a good agreement with past studies (55). Hydrodynamic radius of the DNA condensates was also confirmed by analyzing DNA globules Brownian motion by FM (56) (data not shown), which was 144±26 nm and 125±30 nm for K_4S_4 and $(KS)_4$, respectively. The morphology of the compacted DNA altered significantly depending on the octamer sequence. All-or-nothing type of DNA compaction induced by K_4S_4 produced very ordered DNA particles having either toroidal or rod-like morphology (**Figure 4, top**). In earlier experiments (55, 57), theoretical works (58, 59), and computer simulations (57, 60) these DNA morphologies were accounted to as the characteristic compact structures of semi-flexible DNA chain formed when the attraction interactions between DNA segments is weak. In contrast, DNA compaction by stronger condensing agent $(KS)_4$, which induced gradual compaction of DNA into globules (**Figure 2E**), resulted in a formation of DNA condensates with a disordered

morphology (**Figure 4, bottom**). Formation of the irregular condensate is considered to be the straightforward consequence of stronger attractive interactions between DNA segments in a single DNA chain that causes the appearance of kinetically stable DNA loops stabilized by cationic binder. Formation of these DNA loops disrupts ordered DNA folding into toroid or rod condensates and the final morphology appears as compact condensates with entangled DNA chains. TEM images also suggest that difference in the primary structure of oligopeptides may promote either parallel ordering of DNA chain during folding (K_4S_4) or random cross-linking ($(KS)_4$). The observed striking morphological difference between DNA condensates formed by oligopeptides suggests further difference in their transfection characteristics of the compacted DNA particles.

Earlier studies demonstrated that DNA compaction mechanism is closely related to DNA accessibility by enzymes that affects DNA biological functions (34, 61, 62). In order to make clear the effect of an octamer structure on the accessibility of DNA to enzymes during DNA compaction, we investigated the transcriptional activity of the DNA at different concentrations of oligopeptides. **Figure 5A** shows the dependence of LambdaGEM-11 DNA (*ca.* 43 kbp) transcriptional activity in solutions containing transcription buffer and various concentrations of K_4S_4 or $(KS)_4$.

Transcriptional activity was monitored by fluorescence spectroscopically using an assay described in details elsewhere (34). Increase in concentration of either peptide octamer in solution of long DNA resulted in the inhibition of DNA transcription (**Figure 5B**). The concentration of peptide octamers at which the complete inhibition of DNA transcription activity occurred, correlated with DNA compaction potential of oligopeptide: $(KS)_4$ octamer that compacted DNA at lower concentrations than K_4S_4, completely suppressed DNA transcription at *ca.* 10-fold lower concentration than K_4S_4. Furthermore, transcription inhibition curves (**Figure 5B**) reveal notable correlation with DNA compaction mechanism.

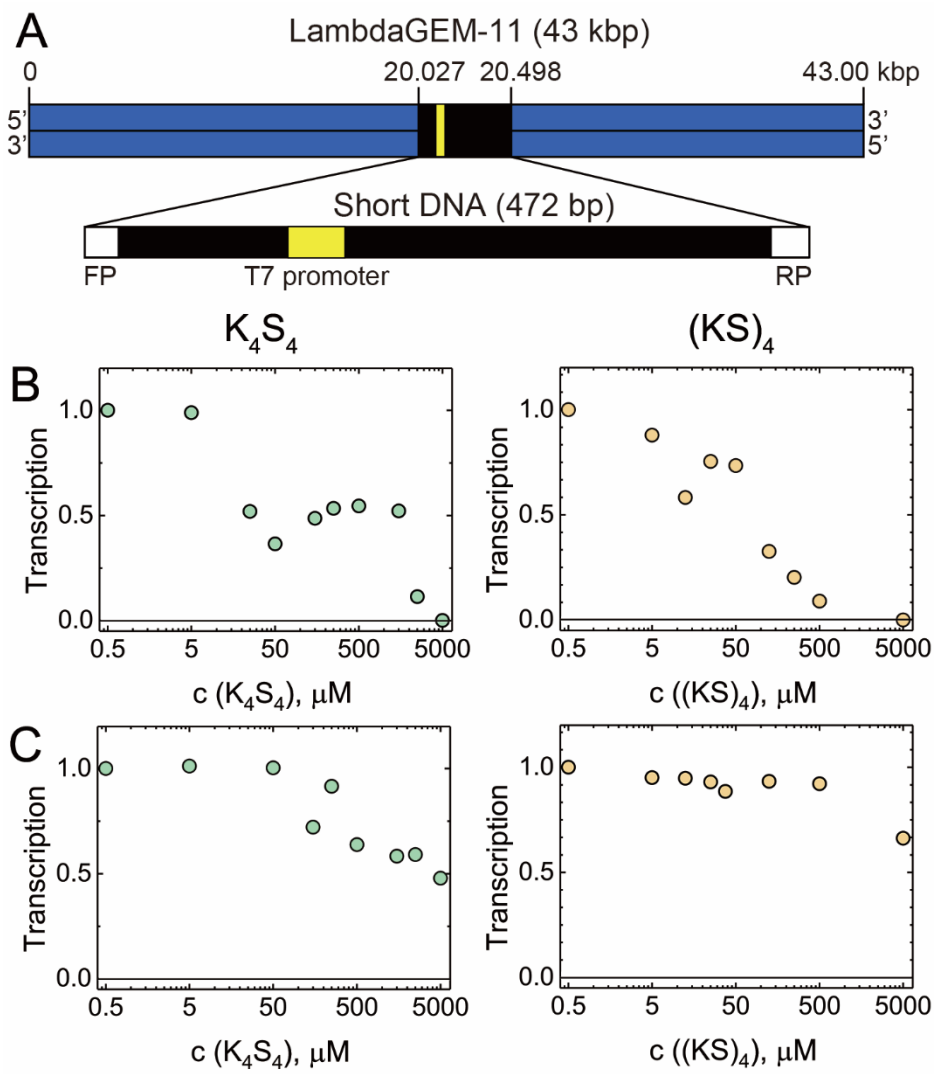

Figure 5. DNA transcription in solution of peptide octamers. A. Map of the LambdaGEM insertion vector DNA and a map of short DNA in which the position the T7 promoter and the forward and reverse primers for PCR are indicated. Numbers above the map indicate the base pair number of the (+) strand **B-C.** Relative transcriptional activity of T7 RNA polymerase determined as an amount of RNA transcribed from LambdaGEM DNA (**B**) and a 472-mer short DNA fragment (**C**), as a function of K_4S_4 or $(KS)_4$ concentrations. The values were normalized by the values of relative transcriptional activity of T7 RNA in solution at the lowest concentration of octamers (0.5 μM). The maximal statistical error of DNA transcription activity measurements estimated from representative triplicated experiments was below 50%.

Continuous compaction of DNA by $(KS)_4$ was consistent with a gradual inhibition of DNA transcription. In the case of the abrupt compaction of DNA by K_4S_4, significant transcriptional activity remained over a long range of K_4S_4 concentrations and was finally suppressed in a very cooperative manner.

The difference between K_4S_4 and $(KS)_4$ in the transcription activity inhibition was manifested only for long DNA molecules, whereas there was only minor effect on the transcription activity of short 147 bp DNA fragments (**Figure 5C)**. In contrast to long DNA, only a slight inhibition of DNA transcription activity was found for both K_4S_4 and $(KS)_4$. Interestingly, stronger inhibition of short DNA transcription was found for K_4S_4 despite its stronger DNA binding potential observed by FM. This difference suggests that aggregation of short DNA molecules is fundamentally different from the compaction of genomic DNA. Here, it is to be noted that 147 bp corresponds to persistence length of double-stranded DNA (20,37). In other words, such short DNA molecules behave as rigid rods, therefore, looping is arrested and toroidal or globular structures cannot be generated on the level of single molecules. In aggregates of short DNA, a large part of DNA is still accessible to polymerase and the transcriptional activity well survives even at high concentrations of oligopeptides. Thus, the change of the DNA length scale should have important consequences to the scenario of DNA condensation including compaction, shrinkage, aggregation, segregation, etc., and has further effect on DNA biological functions (20, 37, 63).

Conclusions

We have shown that difference in amino acids sequence order in an oligopeptide can cause dramatic changes in the mechanism of long DNA compaction and DNA bioactivity. The effect of amino acid sequence alteration in oligopeptide of the same charge on the attraction between DNA helices in the condensed state was reported in past literature (30), but only slight or no effect of sequence change on DNA helices attraction was found. Importantly, the effect of sequence on higher-order conformational behavior of long DNA molecules has never been shown. In this contribution we demonstrated that consequences of a slight changes in oligopeptide sequence may affect the whole process of DNA compaction. In the proposed

model, originated from geometry matching of DNA phosphate groups to oligopeptide amines, weakly binding oligopeptide compacted DNA at higher concentrations and by all-or-nothing mechanism, while strongly binding oligopeptide induced gradual transition of DNA from coil to globules completed at lower concentrations of the peptide octamer. Consequently, the compaction mechanism determined the morphology of DNA condensates that were more ordered for all-or-none type of compaction and largely disrupted for the continuous one. In relation to the morphological change of DNA condensates, it is important to make clear how the degree of charge neutralization induced by various cationic species as well as their binding constant concerns with the morphological change (64, 65), as the next step of the present investigation.

Finally, DNA compaction mechanism had a pronounced effect on DNA transcription inhibition scenario that was either continuous or abrupt and notably correlated with DNA compaction mechanism. We thus conclude that a slight difference in the primary structure of DNA-binding polypeptide or its part may cause a marked effect on DNA higher-order structure, DNA compaction mechanism, and morphology of DNA-peptide complexes, that may significantly alter DNA bioactivity.

Authors contribution

T.A. and N.H. designed the research. H.H performed the experiments. T.K. supported TEM observation. H.Y., K.K. and S.M. partially supported the analysis of data and the research. K.Y. supported the discussion about all of the results and improvement of the manuscript. A.Z. and T.A. wrote the manuscript.

Acknowledgement

This work was supported in part by KAKENHI (grant number 17K05611).

References

1. Toma, A. C., M. de Frutos, F. Livolant, and E. Raspaud. 2009. DNA condensed by protamine: a "short" or "long" polycation behavior. Biomacromolecules 10:2129-2134.
2. Korolev, N., A. Allahverdi, A. P. Lyubartsev, and L. Nordenskiold. 2012. The polyelectrolyte properties of chromatin. Soft Matter 8:9322-9333.
3. Luger, K., A. W. Mader, R. K. Richmond, D. F. Sargent, and T. J. Richmond. 1997. Crystal structure of the nucleosome core particle at 2.8 A resolution. Nature 389:251-260.
4. Schiessel, H. 2003. The physics of chromatin. J. Phys. Condens. Mat. 15:R699-R774.
5. Kalashnikova, A. A., M. E. Porter-Goff, U. M. Muthurajan, K. Luger, and J. C. Hansen. 2013. The role of the nucleosome acidic patch in modulating higher order chromatin structure. J R Soc Interface 10.
6. Slama-Schwok, A., K. Zakrzewska, G. Leger, Y. Leroux, M. Takahashi, E. Kas, and P. Debey. 2000. Structural changes induced by binding of the high-mobility group I protein to a mouse satellite DNA sequence. Biophys J 78:2543-2559.
7. Malarkey, C. S., and M. E. A. Churchill. 2012. The high mobility group box: the ultimate utility player of a cell. Trends Biochem Sci 37:553-562.
8. Ganji, M., M. Docter, S. F. Le Grice, and E. A. Abbondanzieri. 2016. DNA binding proteins explore multiple local configurations during docking via rapid rebinding. Nucleic Acids Res 44:8376-8384.
9. Murugesapillai, D., M. J. McCauley, L. J. Maher, 3rd, and M. C. Williams. 2017. Single-molecule studies of high-mobility group B architectural DNA bending proteins. Biophys Rev 9:17-40.
10. Luo, D., and W. M. Saltzman. 2000. Synthetic DNA delivery systems. Nat Biotechnol 18:33-37.
11. Saccardo, P., A. Villaverde, and N. Gonzalez-Montalban. 2009. Peptide-mediated DNA condensation for non-viral gene therapy. Biotechnology Advances 27:432-438.
12. Kabanov, A. V., and V. A. Kabanov. 1995. DNA Complexes with Polycations for the Delivery of Genetic Material into Cells. Bioconjugate Chem 6:7-20.
13. Kabanov, V. A., V. G. Sergeyev, O. A. Pyshkina, A. A. Zinchenko, A. B. Zezin, J. G. H. Joosten, J. Brackman, and K. Yoshikawa. 2000. Interpolyelectrolyte complexes formed by DNA and astramol poly(propylene imine) dendrimers. Macromolecules 33:9587-9593.

14. Gaweda, S., M. C. Moran, A. A. C. C. Pais, R. S. Dias, K. Schillen, B. Lindman, and M. G. Miguel. 2008. Cationic agents for DNA compaction. J Colloid Interf Sci 323:75-83.
15. Vijayanathan, V., T. Thomas, and T. J. Thomas. 2002. DNA nanoparticles and development of DNA delivery vehicles for gene therapy. Biochemistry-Us 41:14085-14094.
16. Plank, C., M. X. Tang, A. R. Wolfe, and F. C. Szoka. 1999. Branched cationic peptides for gene delivery: Role of type and number of cationic residues in formation and in vitro activity of DNA polyplexes (vol 10, pg 322, 1999). Hum Gene Ther 10:2272-2272.
17. Huang, D., N. Korolev, K. D. Eom, J. P. Tam, and L. Nordenskiold. 2008. Design and biophysical characterization of novel polycationic epsilon-peptides for DNA compaction and delivery. Biomacromolecules 9:321-330.
18. Teif, V. B., and K. Bohinc. 2011. Condensed DNA: condensing the concepts. Prog Biophys Mol Biol 105:208-222.
19. Estevez-Torres, A., and D. Baigl. 2011. DNA compaction: fundamentals and applications. Soft Matter 7:6746-6756.
20. Zinchenko, A. 2016. DNA conformational behavior and compaction in biomimetic systems: Toward better understanding of DNA packaging in cell. Adv Colloid Interface Sci 232:70-79.
21. Joyeux, M. 2015. Compaction of bacterial genomic DNA: clarifying the concepts. J Phys Condens Matter 27:383001.
22. Wilson, R. W., and V. A. Bloomfield. 1979. Counter-Ion-Induced Condensation of Deoxyribonucleic Acid - Light-Scattering Study. Biochemistry-Us 18:2192-2196.
23. Manning, G. S. 1978. Molecular theory of polyelectrolyte solutions with applications to electrostatic properties of polynucleotides. Q. Rev. Biophys. 11:179-246.
24. Ito, M., A. Sakakura, N. Miyazawa, S. Murata, and K. Yoshikawa. 2003. Nonspecificity induces chiral specificity in the folding transition of giant DNA. J Am Chem Soc 125:12714-12715.
25. DeRouchey, J., B. Hoover, and D. C. Rau. 2013. A comparison of DNA compaction by arginine and lysine peptides: a physical basis for arginine rich protamines. Biochemistry-Us 52:3000-3009.
26. Akitaya, T., A. Seno, T. Nakai, N. Hazemoto, S. Murata, and K. Yoshikawa. 2007. Weak interaction induces an ON/OFF switch, whereas strong interaction causes gradual

change: Folding transition of a long duplex DNA chain by poly-L-lysine. Biomacromolecules 8:273-278.

27. Mann, A., G. Thakur, V. Shukla, A. K. Singh, R. Khanduri, R. Naik, Y. Jiang, N. Kalra, B. S. Dwarakanath, U. Langel, and M. Ganguli. 2011. Differences in DNA condensation and release by lysine and arginine homopeptides govern their DNA delivery efficiencies. Mol Pharm 8:1729-1741.
28. Mann, A., R. Richa, and M. Ganguli. 2008. DNA condensation by poly-L-lysine at the single molecule level: role of DNA concentration and polymer length. J Control Release 125:252-262.
29. DeRouchey, J., B. Hoover, and D. C. Rau. 2013. A Comparison of DNA Compaction by Arginine and Lysine Peptides: A Physical Basis for Arginine Rich Protarnines. Biochemistry-Us 52:3000-3009.
30. DeRouchey, J. E., and D. C. Rau. 2011. Role of amino acid insertions on intermolecular forces between arginine peptide condensed DNA helices: implications for protamine-DNA packaging in sperm. J Biol Chem 286:41985-41992.
31. Sohn, B.-K., H. S. Lee, H. Kang, S.-W. Lee, H. Kim, J. Yoo, A. Aksimentiev, J.-M. Kee, and W. Ma. 2018. Sequence-dependent DNA condensation as a driving force of DNA phase separation. Nucleic Acids Res 46:9401-9413.
32. Plank, C., M. X. Tang, A. R. Wolfe, and F. C. Szoka, Jr. 1999. Branched cationic peptides for gene delivery: role of type and number of cationic residues in formation and in vitro activity of DNA polyplexes. Hum Gene Ther 10:319-332.
33. Atherton, E., M. J. Gait, R. C. Sheppard, and B. J. Williams. 1979. The polyamide method of solid phase peptide and oligonucleotide synthesis. Bioorganic Chemistry 8:351-370.
34. Akitaya, T., K. Tsumoto, A. Yamada, N. Makita, K. Kubo, and K. Yoshikawa. 2003. NTP concentration switches transcriptional activity by changing the large-scale structure of DNA. Biomacromolecules 4:1121-1125.
35. Kinjo, A. R., and K. Nishikawa. 2006. CRNPRED: highly accurate prediction of one-dimensional protein structures by large-scale critical random networks. Bmc Bioinformatics 7.
36. Yoshikawa, K., and Y. Matsuzawa. 1995. Discrete phase transition of giant DNA dynamics of globule formation from a single molecular chain. Physica D 84:220-227.
37. Bloomfield, V. A. 1996. DNA condensation. Curr Opin Struc Biol 6:334-341.

38. Melnikov, S. M., V. G. Sergeyev, and K. Yoshikawa. 1995. Discrete Coil-Globule Transition of Large DNA Induced by Cationic Surfactant. J Am Chem Soc 117:2401-2408.
39. Zinchenko, A. A., V. G. Sergeyev, K. Yamabe, S. Murata, and K. Yoshikawa. 2004. DNA compaction by divalent cations: Structural specificity revealed by the potentiality of designed quaternary diammonium salts. Chembiochem 5:360-368.
40. Takahashi, M., K. Yoshikawa, V. V. Vasilevskaya, and A. R. Khokhlov. 1997. Discrete coil-globule transition of single duplex DNAs induced by polyamines. J Phys Chem B 101:9396-9401.
41. Yoshikawa, Y., and K. Yoshikawa. 1995. Diaminoalkanes with an Odd Number of Carbon-Atoms Induce Compaction of a Single Double-Stranded DNA Chain. Febs Lett 361:277-281.
42. Vijayanathan, V., T. Thomas, A. Shirahata, and T. J. Thomas. 2001. DNA condensation by polyamines: A laser light scattering study of structural effects. Biochemistry-Us 40:13644-13651.
43. Zinchenko, A. A., M. Tanahashi, and S. Murata. 2012. Photochemical Modulation of DNA Conformation by Organic Dications. Chembiochem 13:105-111.
44. Muramatsu, A., Y. Shimizu, Y. Yoshikawa, W. Fukuda, N. Umezawa, Y. Horai, T. Higuchi, S. Fujiwara, T. Imanaka, and K. Yoshikawa. 2016. Naturally occurring branched-chain polyamines induce a crosslinked meshwork structure in a giant DNA. J Chem Phys 145.
45. Esadze, A., C. Chen, L. Zandarashvili, S. Roy, B. M. Pettitt, and J. Iwahara. 2016. Changes in conformational dynamics of basic side chains upon protein-DNA association. Nucleic Acids Res 44:6961-6970.
46. Kornyshev, A. A., D. J. Lee, S. Leikin, and A. Wynveen. 2007. Structure and interactions of biological helices. Rev Mod Phys 79:943-996.
47. Kornyshev, A. A., and S. Leikin. 1999. Electrostatic zipper motif for DNA aggregation. Phys Rev Lett 82:4138-4141.
48. Schellman, J. A., and N. Parthasarathy. 1984. X-Ray-Diffraction Studies on Cation-Collapsed DNA. J Mol Biol 175:313-329.
49. Cherstvy, A. G., and V. B. Teif. 2013. Structure-driven homology pairing of chromatin fibers: the role of electrostatics and protein-induced bridging. J Biol Phys 39:363-385.

50. Yoshikawa, K., M. Takahashi, V. V. Vasilevskaya, and A. R. Khokhlov. 1996. Large discrete transition in a single DNA molecule appears continuous in the ensemble. Phys. Rev. Lett. 76:3029-3031.
51. Post, C. B., and B. H. Zimm. 1979. Internal Condensation of a Single DNA Molecule. Biopolymers 18:1487-1501.
52. Post, C. B., and B. H. Zimm. 1982. Light-Scattering Study of DNA Condensation - Competition between Collapse and Aggregation. Biopolymers 21:2139-2160.
53. Nayvelt, I., T. Thomas, and T. J. Thomas. 2007. Mechanistic differences in DNA nanoparticle formation in the presence of oligolysines and poly-L-lysine. Biomacromolecules 8:477-484.
54. Nishio, T., Y. Yoshikawa, W. Fukuda, N. Umezawa, T. Higuchi, S. Fujiwara, T. Imanaka, and K. Yoshikawa. 2018. Branched-Chain Polyamine Found in Hyperthermophiles Induces Unique Temperature-Dependent Structural Changes in Genome-Size DNA. Chemphyschem 19:2299-2304.
55. Hud, N. V., and I. D. Vilfan. 2005. Toroidal DNA condensates: Unraveling the fine structure and the role of nucleation in determining size. Annu. Rev. Bioph. Biom. 34:295-318.
56. Matsumoto, M., T. Sakaguchi, H. Kimura, M. Doi, K. Minagawa, Y. Matsuzawa, and K. Yoshikawa. 1992. Direct Observation of Brownian-Motion of Macromolecules by Fluorescence Microscope. J Polym Sci Pol Phys 30:779-783.
57. Noguchi, H., S. Saito, S. Kidoaki, and K. Yoshikawa. 1996. Self-organized nanostructures constructed with a single polymer chain. Chem Phys Lett 261:527-533.
58. Cherstvy, A. G. 2005. Structure of DNA toroids and electrostatic attraction of DNA duplexes. J Phys-Condens Mat 17:1363-1374.
59. Cherstvy, A. G., and E. P. Petrov. 2014. Modeling DNA condensation on freestanding cationic lipid membranes. Phys Chem Chem Phys 16:2020-2037.
60. Cortini, R., B. R. Care, J. M. Victor, and M. Barbi. 2015. Theory and simulations of toroidal and rod-like structures in single-molecule DNA condensation. J Chem Phys 142.
61. Tsumoto, K., F. Luckel, and K. Yoshikawa. 2003. Giant DNA molecules exhibit on/off switching of transcriptional activity through conformational transition. Biophys Chem 106:23-29.

62. Yamada, A., K. Kubo, T. Nakai, K. Yoshikawa, and K. Tsumoto. 2005. All-or-none switching of transcriptional activity on single DNA molecules caused by a discrete conformational transition. Appl Phys Lett 86.
63. Yoshikawa, Y., Y. Suzuki, K. Yamada, W. Fukuda, K. Yoshikawa, K. Takeyasu, and T. Imanaka. 2011. Critical behavior of megabase-size DNA toward the transition into a compact state. J Chem Phys 135.
64. Yamasaki, Y., Y. Teramoto, and K. Yoshikawa. 2001. Disappearance of the negative charge in giant DNA with a folding transition. Biophys J 80:2823-2832.
65. Kashiwagi, Y., T. Nishio, M. Ichikawa, C.-Y. Shew, N. Umezawa, T. Higuchi, K. Sadakane, Y. Yoshikawa, and K. Yoshikawa. 2018. Repulsive/attractive interaction among compact DNA molecules as judged through laser trapping: difference between linear- and branched-chain polyamines. Colloid Polym Sci.